ELSEVIER

Progress in Organic Coatings 62 (2008) 313–320

PROGRESS IN ORGANIC COATINGS

www.elsevier.com/locate/porgcoat

# The interaction of modern sunscreen formulations with surface coatings

Philip J. Barker *, Amos Branch

*BlueScope Steel Research, P.O. Box 202, Port Kembla, New South Wales 2505, Australia*

Received 22 August 2007; received in revised form 6 November 2007; accepted 16 January 2008

**Abstract**

An aggressive, photocatalytically initiated, free-radical degradation mechanism promoted by specific components of modern sunscreen formulations is proposed for appearance of unsightly defects on prepainted steel sheets installed in roofing applications. The effect has been confirmed and reproduced in both laboratory and exterior exposure tests. X-ray diffraction (XRD) studies reveal the presence of a potent photocatalyst in several sunscreen formulations. Electron spin resonance (ESR) studies confirm the photocatalytic activity through monitoring production of hydroxyl radicals, $HO^{\bullet}$, using the spin trapping technique. The model shows that surface coatings with an inherent roughness are highly susceptible to this effect. In practical terms, it is estimated that the weathering (in terms of deterioration of appearance properties) of the coating has been accelerated 100-fold by this photocatalytic degradation mechanism. Benchmark surface coatings for this application sector, based upon 'fluoropolymer' technologies, are also severely damaged in a short space of time.


*Keywords:* Coil coatings; Polymer degradation; Photocatalysis; Free-radicals; Sunscreen

## 1. Introduction

In this communication, the effects that certain sunscreen components have in causing appearance defects on surface coatings of various types employed in manufactured articles for exterior applications are highlighted. While the detail of this paper pertains to the effects as they relate to prepainted steel roofing and fencing products, there are other surface coatings sectors where similar effects could be observed.

Recently, an increasing incidence of unsightly appearance defects upon relatively newly installed prepainted steel roofs has been noted (see Section 4.1). The defects appeared to arise from accidental splashes of liquid (blotchy appearance) or inadvertent handling (finger marks, footprints) on the surface of the installed roof. The damage to the painted surface is extensive where contact with the material causing the defect has occurred, but directly adjacent, the main body of the installation exhibits normal performance. In a recent example, the main body of the roof after 18 months exhibited normal performance, with over 95% of initial gloss retained, but in the areas where contact had occurred, 0% of initial gloss was retained, this gloss differential leading to an ugly, patchy appearance. In normal service for this type of product, this degree of gloss loss would be reached after 15 years! Moreover, the effect was so localized that where pressure contact had occurred, individual fingerprints and the sole prints of shoes were clearly delineated. Observation of the effect[1] was particularly surprising in Australia where these types of surface coatings are formulated for optimum durability (in terms of gloss retention, colour change and chalk rating), in an aggressive environment (elevated temperatures, high UV), for a high quality market sector (domestic roofing). The effect is apparently not restricted to a particular coating chemistry and this paper also indicates that the effect can be observed upon a range of other highly durable coating types, including polyester–melamine, hindered amine (HALS) stabilised polyester–melamine, polyester–urethane and even 'fluoropolymer' (polyvinylidene difluoride, PVDF-based) surface coatings.

In an attempt to minimize the potential future impact of this failure mode upon coil-coated products in exterior applications, a study was initiated to determine the cause of the problem and to create a 'mechanistic model' for the observed effect. This paper describes the initial results of the study, revealing that the effect observed upon the roofing installations in question is not due to any deficiency inherent in the paint system or roofing product. The effect is due to the aggressive photocatalytic activity of

* Corresponding author. Tel.: +61 2 42523266; fax: +61 2 42523120.
*E-mail address:* Philip.Barker@bluescopesteel.com (P.J. Barker).

[1] See Supplementary data for pictorial examples.

0300-9440/$ – see front matter © 2008 Elsevier B.V. All rights reserved.
doi:10.1016/j.porgcoat.2008.01.008

components in certain types of sunscreen, which by poor handling practices or inadvertent splashing, have come in contact with the product, most likely during installation.

Various types of sunscreen have been identified as the most probable cause for the failure, specifically those sunscreens containing nano-particulate, photocatalytic grades of the semiconducting metal oxides titanium dioxide, $TiO_2$, and zinc oxide, ZnO. Indeed, it was found by X-ray diffraction (XRD) and electron spin resonance (ESR) that a 'UV absorber' employed in several formulations appears to be of similar composition and photocatalytic activity to the IUPAC standard $TiO_2$ photocatalyst [1].

The desirable applications of titanium dioxide in the surface coatings sector are many, varied, and cover a complete spectrum of the photocatalytic activity of this important material: the most inactive grades are highly durable white pigments for exterior applications; the most active grades are employed in self-cleaning and anti-bacterial applications. A recent study [2] has highlighted in considerable detail how particle size, various surface treatments and dispersion of several 'nano' and 'pigmentary' grades of titania particles affect the degradation and stabilization of polymers and coatings. However, to our knowledge, this is the first report detailing the direct consequences of photocatalytic destruction of highly durable surface coatings, in-service, through direct contact with other substances (sunscreens) containing these nanomaterials.

In addition, the mechanistic model for the action of these sunscreen components is described. This model is relevant to any surface coatings to which an inherent roughness has been imparted to achieve a desired performance or aesthetic attribute. These coatings may be particularly susceptible to this type of damage.

## 2. Experimental

### 2.1. Sunscreens

In Australia, manufacturers of sunscreens are obliged to disclose full details and the concentration of active ingredients on the packaging. Other ingredients in terms of preservatives and solvents are not always disclosed. A survey of the packaging of 35 commercial sunscreens was conducted and from this overview, a core set of 10 sunscreens exhibiting key compositional variables were selected for study. Table 1 summarizes the compositional characteristics of the sunscreens. Sunscreens were purchased in pharmacies, 'over-the-counter', in November 2006.

### 2.2. Exterior exposure testing

Sunscreens were applied to flat test panels of a prepainted steel product. The panels were part of normal coil paint line production (i.e. not laboratory prepared). The test panels initially measured 250 mm × 100 mm. Sunscreens were applied with a #10 wire-wound drawdown bar: 3 g of sunscreen was placed halfway along the length of the test panel, then drawn down with the bar, giving panels with an uncovered top half, and a bottom half coated with around 13 μm of wet sunscreen. The panels were mounted lengthwise on an insulated exposure rack, designed to enable the test panels to reach in-service temperatures, at Port Kembla, NSW and exposed over the Australian summer. After 6 weeks a 30 mm wide strip was cut off each panel for testing, while the remainder of the panel was remounted on the exposure rack. After 12 weeks a further strip was removed, with the remaining strip allowed to remain on the rack for future testing. Trends were indicated after 6 weeks and clear differentiation of affected samples was confirmed after only 12 weeks of exposure.

Table 1
Identification and composition of sunscreens employed in the study

| Sunscreen | Inorganic components | Organic components[a] |
|---|---|---|
| A | None | OMC (8%); BMDBM (2%); 4-MBC (3%) |
| B | None | OMC (7.5%); 4-MBC (4%); OT (3%); BT (2%) |
| C | None | OMC (7.5%); BMDBM (3%); 4-MBC (3%); OB (3%) |
| D | None | OMC (7%); BMDBM (4%); OB (3%) |
| E | $TiO_2$ (5%) | OMC (8%); BMDBM (4%); 4-MBC (4%) |
| F | $TiO_2$ (2.5%) | OMC (7.5%) |
| G | $TiO_2$ (4%) | OMC (7%); BMDBM (4%) |
| H | $TiO_2$ (9%) | OMC (3%); BMDBM (3%) |
| I | $TiO_2$ (5%) | BMDBM (2.5%) |
| J | ZnO (3%) | OMC (3%); 4-MBC (1%) |

[a] The common organic components are (trivial names)—OMC: octylmethoxy cinnamate; BMDBM: butylmethoxydibenzoylmethane; 4-MBC: 4-methylbenzylidene camphor; OB: oxybenzone; BT: bemotrizinol; OT: octyltriazone.

### 2.3. Laboratory durability testing—'accelerated weathering'

Laboratory 'accelerated weathering' was conducted using a Q-Sun Xe-1S device (Q-Panel Company, Cleveland, OH). A cyclic testing regime was devised to optimise conditions for photocatalysis to occur: a light cycle of 7.5 h (irradiance 750 mW $cm^{-2}$ at a temperature of 80 °C) was followed by 0.5 h of light and water-spray (at 35 °C); after the 'light + spray' period was complete, a 3.5 h dark period at 50 °C was followed by a 0.5 h period of 'dark + spray'. The total 12 h cycle was run continuously for a 20-day period.

This method was not based upon a previously published test cycle, although the '8 h on/4 h off' light regime bears obvious similarity to ASTM D4587, cycle 1 [3]. It has several facets relevant to both testing of photocatalyst samples in general and to exposure in the harshest Australian test conditions. The Q-Sun device employs a Xenon arc lamp for irradiation and this is critical when studying both coil coatings for roofing applications and $TiO_2$ photocatalysis, as here. Unlike UV testing methods that employ 'monochromatic' radiation from fluorescent tubes, the spectrum of the xenon arc (with Daylight Filter) not only closely matches the sunlight spectrum (Miami, Florida) in the

UVB and UVA regions [4], but also includes the visible and infrared regions of the spectrum. Thus, the critical wavelengths encompassing the absorbance profile of both anatase and rutile phases of $TiO_2$ are included. The 30 min 'spray' cycles are also significant, with the spray at the end of the light cycle able to remove debris from the exposed sample surface, while the spray at the end of the dark cycle provides more moisture to induce photocatalysis when the light cycle commences.

### 2.4. Test sample characteristics

The test panels for the exterior exposure testing were of a dark blue colour and the topcoat paint employed was a highly durable aromatic di-acid based branched polyester, cross-linked with a melamine-formaldehyde cross-linking agent. Pigments employed in the formulation were typical highly durable metal oxide and mixed metal oxides. By keeping this test sample to a single commercial system, the action of different sunscreens could be clearly seen.

Having realised that some sunscreens were highly active, it was decided to test the effect of a single active sunscreen, H, upon different types of durable surface coating when subjected to Q-Sun testing. The test samples included: a control sample similar to that employed in the exterior exposure testing (I); a fluoropolymer, PVDF-based topcoat of the same colour (II); an alternative dark blue polyester–melamine system (III), the alternative resin system with 2% (resin basis) HALS added (IV, with Tinuvin® 123, CIBA Specialty Chemicals), the alternative resin system cross-linked with a durable, 1-pack 'urethane' cross-linking system chemically based upon the isophoronedi–isocyanate (IPDI) trimer (V, with DESMODUR®BL4265, Bayer MaterialScience). Panels for Q-Sun testing were cut to a size of 20.5 cm × 5.0 cm and sunscreen H was applied, as before, to the bottom half of each panel.

### 2.5. Preparation of panels for gloss measurement

In order to assess the panels for a meaningful gloss determination, cleaning of the weathered sunscreen debris from the lower portion of each cut strip was necessary. With a soft bristle brush, debris was first removed under warm (∼40 °C) running water. A dilute detergent solution and soft paper towel was then employed to gently rub the surface for 1 min, the panel was rinsed then placed in a rack to air-dry. The samples were then measured using a 60° gloss meter (Byk-Gardner).

### 2.6. Separation of sunscreen components

To separate the active organics and inorganics from the sunscreen a simple method based on solvent extraction was used.

2–3 g of the sunscreen was measured into a 50 ml centrifuge tube along with 30 ml of hexane. The mixture was then shaken and centrifuged (Jouan Centrifuge 7000 rpm, 2 min). This resulted in a hexane solution containing the active organics that could be decanted, filtered and then evaporated to give a clear organic phase. 30 ml of ethanol was added to the residue left at the bottom of the tube. After shaking and centrifuging, this extracted the remaining organics into a solution that could again be decanted leaving only inorganic components and surfactants as residue. 30 ml of water was then added and the mixture shaken, centrifuged and decanted a third time, effectively removing the surfactants from the mixture. The inorganic components were washed with successive aliquots of acetone and dried.

The separation of the inorganics was confirmed by X-ray diffraction to identify the crystalline phases present.

### 2.7. XRD analysis

X-ray diffraction measurements were obtained on a Siemens D5000 diffractometer operating at 45 kV and 40 mA, employing Cu Kα radiation and using a two-circle goniometer in a Bragg–Brentano arrangement. The program "VisualXRD" was used to control the scan parameters and to collect data of diffraction intensity. This data was plotted as a variable versus the $2\theta$ angle. A commercial software package (Diffraction Technologies Pty. Ltd., Traces Version 4.2) was used to smooth the data and to identify the peaks of the plotted data. The peak heights and positions were compared with a database [5] for identification of phases present in the sample.

### 2.8. ESR data

ESR data was obtained on a Bruker ESP300E spectrometer operating in the X-band region of the microwave spectrum. For the photocatalytic activity assessment, an in-house method based upon the well-known spin trapping technique [6] was employed. This technique has recently been used in a study of various (unrelated) aspects of sunscreen chemistry [7] and can be readily adapted to the study of photocatalysis [8] and the photocatalytic activity of nano-materials [9]. In these experiments the technique measures a 'hydroxyl radical generation rate' in liquid samples.

Here, the technique of spin trapping using 5,5-dimethylpyrroline-*N*-oxide (DMPO) as spin trap in de-ionised water was employed. This particular system is uniquely suited to the detection of hydroxyl radicals generated in aqueous solution by photocatalytically active materials [9]. A suspension of the inorganic sample to be tested (0.125 g) is suspended in 200 ml of an aqueous solution of DMPO (∼50 mM), with no other materials present. The sample is vigorously stirred in a quartz-walled batch reactor and then irradiated with light from a high power 1 kW UV source. The light beam passes through, in turn, a 10 cm path length water filter to remove the infrared component of the xenon lamp output, then is attenuated to 30% of normal output intensity with a neutral density filter before finally passing through a 375 nm 'cut-off' filter, only passing UV light *above* 375 nm. Thus, the wavelengths present can excite the semi-conductor phases, anatase and rutile (leading edges of absorption ∼420 and 415 nm, respectively), but not damage the organic component of the system, DMPO, which is known to absorb below 320 nm.

After the light is switched on, small aliquots (1.5 ml) are withdrawn after 1, 3, 5, 7, 10, 15, 20 and 30 min. The solids of each

Table 2
Gloss data for dark blue panels with sunscreen

| Sunscreen | Gloss (6 weeks) | Gloss (12 weeks) |
|---|---|---|
| None | 22 | 20 |
| A | 29 | 27 |
| B | 29 | 26 |
| C | 27 | 26 |
| D | 48 | 17 |
| E | 15 | 4.5 |
| F | 29 | 21.3 |
| G | 3 | 1 |
| H | 4 | 2 |
| I | 4 | 2 |
| J | 16 | 10 |

Initial gloss reading 23 units—exposed at Port Kembla, NSW on insulated racks (45° black-box type, north facing).

sample are spun down at 7000 rpm for 3 min, the supernatant is then removed by pipette and transferred to an ESR 'flat cell' for analysis. Each sample shows the concentration of the hydroxyl radical adduct of DMPO, [DMPO–OH] at that time.

## 3. Results

### 3.1. Exposure panels

Exposure testing took place over the summer months at the BlueScope Steel local exposure site in Port Kembla, NSW. Panels were placed on in-house designed insulated exposure racks facing north at 45°. As described above, after 6 weeks and 12 weeks a 30 mm strip was removed from each panel, and this strip was prepared for gloss reading. Table 2 summarizes the gloss data.

After 6 weeks of exposure, trends were beginning to emerge and these were reinforced when the readings were taken at 12 weeks. In summary, the test panels with 'all organic' components tended to increase in gloss and the surface of the samples was not visibly disfigured. On the other hand, test panels with inorganic components, with the exception of sample F, had all lost gloss, the surfaces of samples E, G, H and I were roughened and disfigured after only 6 weeks exposure. At the 12-week reading, pigment was already being removed from the surfaces of samples G and H during post-exposure clean-up. In addition, these two samples clearly showed individual drawdown bar lines, typical of the 'pressure-point' marking observed on roofing installations.

The fact that semi-conducting metal oxides were a common component of the sunscreens on all the poor performing panels indicated that a photocatalytic mechanism for degradation could be in place. This conclusion is also supported by the fact that this extreme level of damage occurred at a latitude not normally regarded as aggressive for exterior exposure testing—Port Kembla, New South Wales (NSW) is located on a latitude ∼34.5°S whereas the conventional surface coatings durability testing facilities in Australia are at Rockhampton, Queensland (QLD) at 23.5°S or Allunga (QLD) at ∼19.5°S.

### 3.2. Accelerated weathering study of alternative topcoat systems

After 20 days testing in the Q-Sun, panels were removed and prepared for gloss measurement. The results are summarized in Table 3, which shows the original gloss of each sample, the gloss of each sample after 20 days testing (top half of test panel) and the gloss of each sample after 20 days testing with sunscreen H applied (bottom half of panel). The results of this test confirmed the aggressive nature of the component in sample H. The conventional polyester formulations were severely damaged after the test period, while even the fluoropolymer system retained only ∼25% of original gloss, indicating that even this highly durable topcoat system is not immune to this type of damage.

### 3.3. X-ray diffraction studies

To investigate the identity of the semi-conducting solids, the sunscreens were separated and the inorganic components were subjected to XRD analysis to determine the crystal phases. The $TiO_2$ containing materials revealed two distinct phases in different sunscreens. The inorganic components from sample F showed a single rutile phase, as shown in Fig. 1(a) with a major *d*-spacing of 27.5° (2$\theta$). The solids isolated from samples E, G, H and I gave XRD traces similar to that shown in Fig. 1(b), revealing a mixture of anatase and rutile, with anatase dominant, having a major *d*-spacing of 25.3° (2$\theta$).

Attempting to identify the origin of the solids giving XRD patterns from E, G, H and I, an authentic sample of the photocatalyst Degussa AEROXIDE® $TiO_2$ P 25, known to be a mixture of anatase and rutile, was subjected to analysis for comparison with the sunscreen pigments. As can be seen from Fig. 1(c), the spectrum is a very good match for the material isolated from the sunscreens.

Table 3
Gloss data for alternative topcoat systems treated with sample H (see Section 2 for key) and subjected to accelerated weathering

| Sample | Original gloss | No sunscreen | | With sunscreen | |
|---|---|---|---|---|---|
| | | Gloss (20 days) | %Gloss retention | Gloss (20 days) | %Gloss retention |
| I | 18.2 | 15.7 | 86.3 | 1.7 | 9.3 |
| II | 22.9 | 21.8 | 95.2 | 5.5 | 24.0 |
| III | 29.5 | 28 | 94.9 | 2.8 | 9.5 |
| IV | 23.5 | 20.5 | 87.2 | 3.0 | 12.8 |
| V | 23 | 21 | 91.3 | 2.1 | 9.1 |

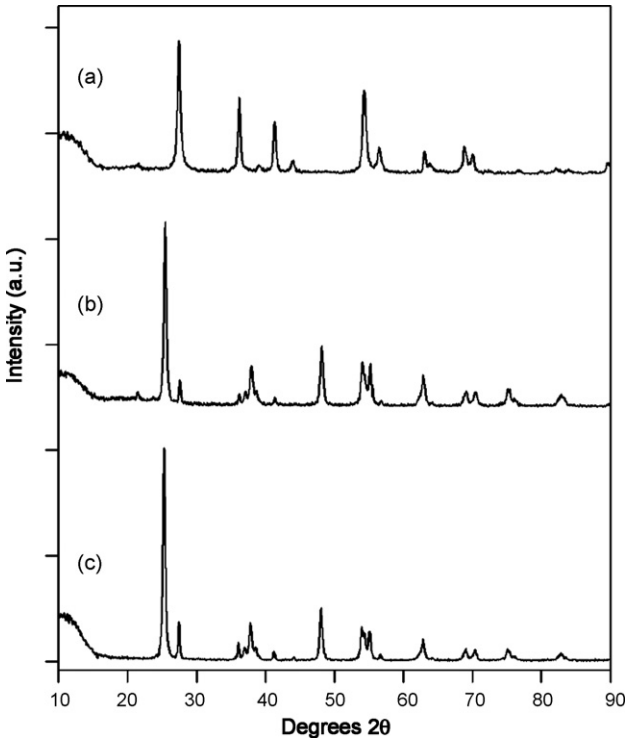


Fig. 1. XRD data from inorganic sunscreen components: (a) shows the single rutile phase from sample F; (b) shows the mixed anatase/rutile phase from samples E, G, H and I; (c) shows the trace from the authentic photocatalyst.

Zinc oxide containing material, isolated from sample J, gave a match for the common zincite ZnO structure.

### *3.4. Photocatalytic activity (PCA) of isolated inorganic components*

In order to demonstrate that the isolated inorganic materials had the potential to exhibit photocatalytic activity, an in-house method, normally used for assessing the PCA of pigment grades of $TiO_2$ in paints, was applied.

In this experiment, samples of the inorganic material isolated from sunscreens F and G were studied. Results from these materials were compared with results from an experimental run with an authentic sample of Degussa AEROXIDE® $TiO_2$ P 25 and a blank run where a solution of DMPO without substrate was subjected to a similar procedure.

Results from a typical experimental run upon the material isolated from sample G, illustrating the development of the spin-adduct, are shown in Fig. 2.

In summary, the data from the 4 experimental runs performed here is collected in Fig. 3, which shows, in bar graph format, the relative intensities of the ESR signals after 30 min irradiation. The pure rutile phase of sunscreen F showed only minor radical generation but clearly the data from sunscreen G, containing the anatase/rutile mixture is similar (within experimental error), to that of the authentic photocatalyst. The blank sample showed no appreciable radical generation.

The robust nature and viability of the experiment is demonstrated in Fig. 4, which shows the irradiation of the blank sample

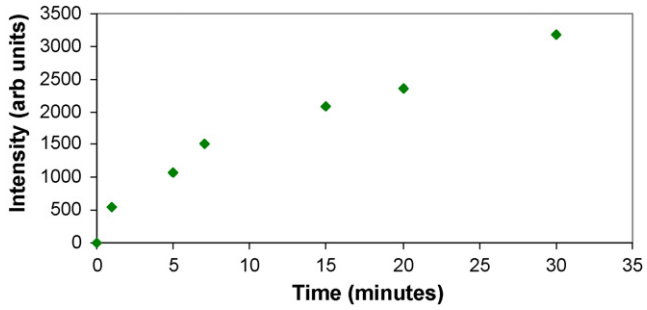


Fig. 2. Typical run from ESR spin trapping experiment, showing development of the [DMPO–OH] spin-adduct with time (this data from sample G).

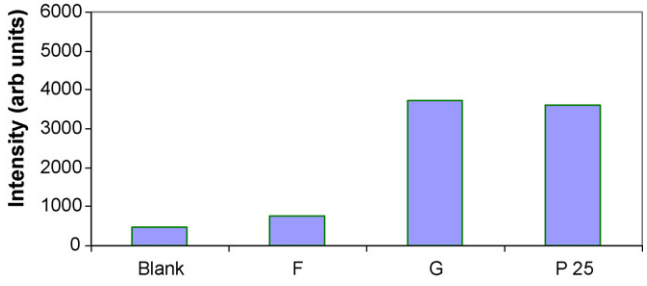


Fig. 3. Bar graph representation of relative ESR spectrum intensities, after 30 min irradiation, in each experiment.

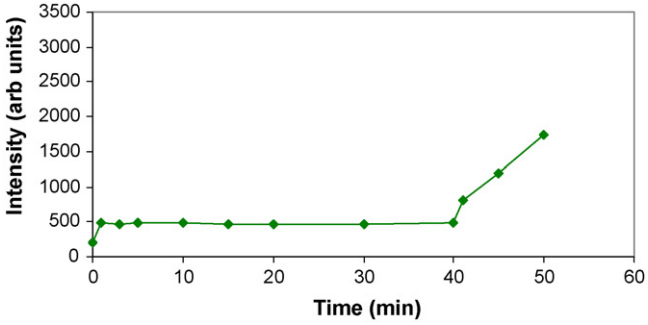


Fig. 4. Blank experimental run involving irradiation of DMPO solution. After 40 min ~0.125 g of authentic photocatalyst was dropped into the reactor (under constant illumination), generation of the spin-adduct was then monitored at 1, 5 and 10 min after the addition.

and where, after 40 min of constant irradiation with no adduct radical formation, ~125 mg of authentic Degussa AEROXIDE® $TiO_2$ P 25 was added to the system. Formation of the DMPO–OH adduct radical commenced immediately after the addition.

Thus, this experimental approach not only confirmed the photocatalytic nature of the inorganic component of sample G, which gave the most severe response in the exposure experiment, but also that it was of similar activity to a known photocatalyst.

## 4. Discussion

### *4.1. General background*

Roofing contractors involved in the installation of prepainted steel roofs are in an obviously 'high-risk' UV exposure situation and the use of sunscreens remains an important part of

the occupational health and safety practice for this specialised part of the workforce. With 'in-house' experience of over 40 years of coil coating for this market and with regular monitoring of product performance upon in-service installations, many hundreds of roof inspections have taken place each year. Until around mid-2006 however, no significantly destructive effects of the many sunscreens available, upon the tens of thousands of coil-coated roofs installed over this period, have been reported. With this experience in mind, the failure is therefore viewed as a recent phenomenon, possibly paralleling the most recent sunscreen developments employing nano-particulate metal oxides as UV blockers. The work reported here has focussed upon detailed review of commercially available sunscreens and sunscreen components, the testing of different generic types, and reproduction and observation of the effect both in the laboratory and under exterior exposure conditions.

### 4.2. Photocatalysis and surface coatings

Detailed review of the background to semi-conductor photocatalysis is beyond the scope of this paper, however, several key aspects of the process and its related effects as applied to surface coatings are worth consideration. Photocatalysis is an inherent property of the two most common crystal forms of titanium dioxide, rutile and anatase. Implication of the photocatalytic process in the degradation of paint binders as it relates to the well-known 'chalking' phenomenon is historically well-known [10]. Understanding both the underlying causes [11] and prevention of the photocatalytic degradation of paint systems by $TiO_2$ through moderation of this effect [12] had been an area of considerable activity, expanding the application of $TiO_2$-based pigments throughout the surface coatings sector. On the other hand, harnessing and maximising the benefits of the photocatalytic process has been a cornerstone of new technology development in surface coatings [13], environmental chemistry [14] and solar cell manufacture [15]. Through its natural abundance, lack of toxicity and relatively low cost, $TiO_2$ is the most widely used material in semi-conductor photocatalysis.

General aspects of the photocatalytic mechanism involve excitation of an electron by light from the valence band to the conduction band in the $TiO_2$ particle, leaving behind a positively charged 'hole'. The electrons and holes migrate to the surface of the particle whereby they can interact with water and oxygen. It is the positively charged hole that reacts with water or surface hydroxyl groups to liberate hydroxyl radicals, while the excited electron reacts with molecular oxygen to give superoxide anion, which can undergo a cascade of further reactions leading to several reactive intermediates (including the hydroxyl radical). The hydroxyl radical is an aggressive oxidant and is able to degrade many types of organic substrate [14] and it is this chemistry that is responsible for the degradation of paint binders. It is widely accepted that despite the slightly lower band gap of rutile (3.1 eV), anatase (band gap 3.3 eV) is both the more highly photocatalytic form of $TiO_2$ and the less durable form of pigmentary $TiO_2$. There are many experimentally established reasons which support the former observation including: the reactivity of anatase/rutile mixtures towards decomposition of chloroacetic acid increases with anatase content [16]; the activity of anatase towards degradation of phenol in aqueous dispersions is more efficient than with rutile [17]; in general, the hydroxyl group density on anatase-based materials is higher than for rutile [18]. Meanwhile, in pigmentary grades, the higher band gap means that anatase absorbs less UV than rutile and the rate of binder photodegradation is therefore greater than for rutile [12]. Many highly durable grades of pigment $TiO_2$ are therefore based upon surface-treated rutile, while many of the highly photocatalytic grades are based upon nano-particulate anatase. ESR spin trapping experiments in our laboratory of the type described in this paper clearly indicate that the difference in hydroxyl radical generation rate between the surface coatings industry benchmark pigment for exterior durability (Dupont TIPURE® R-960) and the IUPAC standard photocatalyst (Degussa AEROXIDE® P 25) is between 6 and 8 orders of magnitude [19].

Whatever surface coating application $TiO_2$ is employed in, suitability of a particular grade for a specific application is critical and success obviously depends upon the knowledge and control of the potential for photocatalytic activity. The physical and chemical properties of both pigmentary and nano-particulate grades of $TiO_2$, with respect to applications in the surface coatings sector, have recently been reviewed in depth [2].

In the case of the effects reported here, control of photocatalytic activity in durable surface coatings has been removed by inadvertent contact of a highly active photocatalyst with the binder of the surface coating and the deleterious effects have become obvious.

### 4.3. A model for sunscreen damage to coil coatings

Having confirmed that the most probable cause of the damage to the coil coatings is a photocatalytic mechanism, involving nano-particulate semi-conducting metal oxides, it is interesting to describe the physical model for the process. The coil coatings employed in prepainted steel for roofing applications are apparently highly susceptible to this mechanism.

Unlike automotive coatings, where high gloss and distinction of image are valued attributes, the market place does not accept similar attributes in roofing products, where extreme glare is unsightly and could cause personal discomfort. Typically, where automotive paint systems are finished with a durable clear-coat, gloss values are over 80 units at 60°. Even high solids solvent borne topcoats for coil coatings would initially have similar values because after cure, pigment settling and film contraction, a nanometer thickness of resin/binder covers the system, imparting high gloss. In order to minimise this effect, many coil coatings employ matting agents in the wet paint formulation. Matting agents have a large particle size (typically 7–10 μm) compared with other pigment components (coloured pigments are typically ∼1 μm, while pigment grades of titanium dioxide are ∼200–300 nm) and are irregular in shape, roughening the surface of the coating and functioning by scattering the incident light. This has the effect of reducing gloss to a degree dependent upon concentration and in normal paints for coil coatings, 3–4% of total pigment loading as matting agent will lead to a cured coating having around 25% of the full gloss unmatted version.

Coil coatings such as those employed here are therefore inherently rough, on the micrometer scale. The inorganic material employed in the sunscreen formulations under scrutiny here, has a mean particle size of 20 nm. This small particle size enables the sunscreen to appear clear, on a surface after application, when well dispersed, but pre-disposes it to become entrained in the roughened surface features of a cured (and matted) coil coating. Accidental splashing of the sunscreen on the roofing sheets during installation can cause the irregular blotchy appearance observed, but entrainment of the photocatalytic particles can be facilitated by application of pressure (as in a fingerprint or the wire of a drawdown bar). Once entrained, the particles are very difficult to remove. This can be demonstrated by considering the gloss results of the totally organic sunscreens, where the gloss is increased upon exposure on the test panels. This observation is attributed to the fact that the organic phase is now trapped in the surface, and cannot be easily removed by rainfall, thus it reduces the roughening effect of the matting agent and imparts an increased gloss. Once entrained in the roughened surface structure of the coil coating, the photocatalytic particles will begin by destroying the rest of the sunscreen matrix, and then commencing decomposition of the coating. Each dew or rainfall event will provide more water, acting as 'fuel' for the photocatalytic cycle [1], and propagating the process indefinitely.

The fact that four of the sunscreens studied here apparently employ the same photocatalytic agent yet the rates of gloss loss are different, as seen for E compared with G, H and I, probably reflects the different initial concentrations and make-up of other non-active components of the sunscreen. The 12-week data demonstrates that E will soon show equivalent appearance to G, H and I. On the other hand, the gloss of sample F remains high after 12 weeks exposure. This observation is attributed to the fact that the rutile phase is inherently less photocatalytic than anatase and that there are several surface-treated rutile phase nano-particulate grades of titanium dioxide developed specifically for the health sector. We do not discount completely the possibility that an effect will be observed at some stage (even the most durable pigment grades of $TiO_2$ for exterior applications 'chalk' eventually) but the particle surface treatment has successfully moderated the photocatalytic activity. This has been confirmed by observation of the decreased hydroxyl radical generation rate in the ESR study.

Much of the discussion here has focussed upon the photocatalytic properties of titanium dioxide components, however, zinc oxide is also a semi-conducting material which can act in a similar manner [14]. This can be seen in the gloss results from sample J where, while not as severe as the $TiO_2$ containing materials, over 50% of the original gloss is lost after 12 weeks, indicating that differential performance is highly probable should contact with surface coatings occur.

### 4.4. Mechanistic implications

The photocatalytic mechanism for polymer degradation is very severe. Unlike conventional degradation kinetics, which depends on a finite concentration of initiator, propagating a series of reactions until termination, the photocatalytic mechanism is exactly as the name implies, catalytic. One particle of titanium dioxide can initiate an infinite number of degradation reactions if oxygen, water and light are available. The radicals initiating the process are hydroxyl radicals, extremely active towards hydrogen abstraction, and aggressive oxidants. The subsequent radical decomposition reactions are accelerated in dark colours upon exterior exposure as the degradation kinetics increase in rate with elevated temperatures. Conventional chain breaking anti-oxidants such as hindered amines would be expected to have little effect upon the degradation processes as they depend upon the classical kinetic model.

Calculations based upon the gloss levels imparted upon exposure at our Port Kembla exposure site indicate that overall, the total deterioration of visible attributes is over 100 times faster than 'conventional' degradation. This calculation is based upon the gloss level of a polyester sample identical in composition to that employed in the test samples A–J, requiring 15 years exposure at Port Kembla to reach the same level of gloss as a sunscreen affected sample does in 6 weeks.

Many UV induced polymer degradation processes are retarded behind glass, because it is able to filter wavelengths below 320 nm. However, the photocatalytic process begins in the visible portion of the spectrum, and thus there could also be implications for interior coatings which are likely to experience contact with the sunscreens containing photocatalytic agents. Moreover, as the coatings discussed here are durable systems for exterior exposure in high temperature and high UV conditions it could be assumed that less durable coating types in general purpose applications could also be severely affected.

## 5. Conclusions

It has been demonstrated that surface coatings in roofing applications are particularly susceptible to unsightly appearance defects that can be caused by the photocatalytic action of specific nano-particulate components of some modern sunscreen formulations. The effect is likely to be observed in other surface coatings[2] where (a) contact with sunscreen is possible and (b) an inherent roughness is desired to achieve specific attributes—this roughness could lead to entrainment of photocatalytic particles leading to appearance problems of the type described here.

The work has shown that the effect is not due to any inherent fault in the coating or coated article, nor was it imparted during processing or manufacture. Relatively simple test procedures are described which producers of surface coated, manufactured products of any description might employ to evaluate the risk to their products. Accelerated weathering machines will reveal the effect in 1–3 weeks of testing, using cycles similar to that described herein. In addition, as the mechanism is photocatalytic, the typical high UV sites employed in the surface coatings sector for exterior exposure testing are not necessary to reproduce the effect. Thus, continuous exposure for up to 12 weeks

[2] See Supplementary data (Fig. 6), for a pictorial example of suspected sunscreen damage to a high gloss automotive surface coating.

in moderate summer sunlight would be expected to reveal the damage imparted by the sunscreens in question.

## Acknowledgements

We thank BlueScope Steel for permission to publish this work. A.B. would like to acknowledge the University of New South Wales Co-op. office and BlueScope Steel for the award of a scholarship. We thank the BlueScope Steel Research Surface Analysis Group for the XRD data. P.J.B. is a partner investigator in the Australian Research Council 'Centre of Excellence for Free Radical Chemistry and Biotechnology'.

## Appendix A. Supplementary data

Supplementary data associated with this article can be found, in the online version, at doi:10.1016/j.porgcoat.2008.01.008.

## References

[1] N. Serpone, A. Salinaro, IUPAC Pure Appl. Chem. 71 (1999) 303.
[2] N.S. Allen, M. Edge, A. Ortega, G. Sandoval, C.M. Liauw, J. Verran, J. Stratton, R.B. McIntyre, Pol. Deg. Stab. 85 (2004) 927.
[3] Annual Book of ASTM Standards, Volume 6.01, D 4587-01, 2002.
[4] Technical Bulletin LU-8009.1, Q-Lab Corporation, Cleveland, OH, 2006.
[5] Powder Diffraction File, International Centre for Diffraction Data, Release, 1998.
[6] F. Gerson, W. Huber, Electron Spin Resonance Spectroscopy of Organic Radicals, Wiley-VCH Verlag, Weinheim, 2003, ISBN: 3-527-30275-1 (Appendix A.1).
[7] V. Brezova, S. Gabcova, D. Dvoranova, A. Stasko, J. Photochem. Photobiol. B: Biol. 79 (2005) 121.
[8] M.A. Grela, M.E.J. Coronel, A.J. Colussi, J. Phys. Chem. 100 (1996) 16940.
[9] G. Wakefield, M. Green, S. Lipscomb, B. Flutter, Mater. Sci. Technol. 20 (2004) 985.
[10] H.G. Volz, G. Kaempf, H.G. Fitzky, A. Klaeren, Photodegradation and photostabilisation of coatings, in: ACS Symposium Series No. 151, ACS, WA, 1981, p. 163.
[11] M.P. Diebold, Surf. Coat. Int. (1995) 250.
[12] M.P. Diebold, Surf. Coat. Int. (1995) 294.
[13] A. Fujishima, K. Hashimoto, T. Watanabe, $TiO_2$ Photocatalysis—Fundamentals and Applications, BKC Inc., Tokyo, 1999, ISBN: 4-939051-03-X.
[14] A. Mills, S. Le Hunte, J. Photochem. Photobiol. A: Chem. 108 (1997) 1.
[15] U. Bach, D. Lupo, M. Graetzel, Nature 395 (1998) 583.
[16] K. Tanaka, M.F.V. Capule, T. Hisanaga, Chem. Phys. Lett. 187 (1991) 73.
[17] A. Sclafani, L. Palmisano, E. Davi, New J. Chem. 14 (1990) 265.
[18] T. Renschler, Eur. Coat. J. (1997) 939.
[19] P.J. Barker, I. Gabriel, unpublished data.